Published by :
http://www.ijert.org

International Journal of Engineering Research & Technology (IJERT)
ISSN: 2278-0181
Vol. 8 Issue 04, April-2019

Design and Analysis of Flapping Wing Unmanned Aerial Vehicle

R. Jagadeesh
Department of Aeronautical Engineering
KCG College of Technology
Chennai, India

S. Madhu Mathi
Department of Aeronautical Engineering
KCG College of Technology
Chennai, India

Dr. K. Vijayaraja
Department of Aeronautical Engineering
KCG College of Technology
Chennai, India

***Abstract*— This project presents the design of a Flapping wing UAV which is inspired by various bird mechanism and its action during flight. In this project, the real actions have been tried to convert into a perfect mechanism in order to get a stable flight manuvering. Biomemic plays a major role in this design. The design has been made CATIA V5 with all the parameters calculated according to the bird selected. The moving mesh analysis is completed with the help of ANSYS 19.0. This UAV can be widely used for surveillance for civilian and military applications.**

***Keywords*—CATIA; ANSYS; flapping; UAV; lift; dynamic; meshing;**

I. INTRODUCTION

The flapping wing aircraft which will produce lift and thrust by the flapping mechanism. Using Bio-mimic various Ornithopter, designs have been suggested for civil and military applications especially for the purpose of surveillance. In this paper, the highly aerodynamic design for flapping wing UAV with advanced specifications have been created. The flapping wing UAV made which can be used for surveillance or reconnaissance of a particular target and also for a specific environment without its own consciousness. The Ornithopter uses battery power, gear mechanism, which enables to increase the number of flaps. We are bringing down the specifications of various birds and trying it to convert it into perfect real time mechanism. As of the first initiative, the basic and operating principles of flight have been studied in order to understand the flapping mechanism.

- For an airplane/ bird to stay at a constant height,

Lift force upwards = Weight force downwards

- For an airplane/bird to stay at a constant speed,

Thrust force forwards = opposing force of Drag
Ease of Use

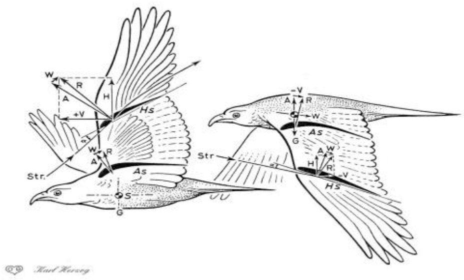

Figure 1 Flight Action of Flapping Wing UAV

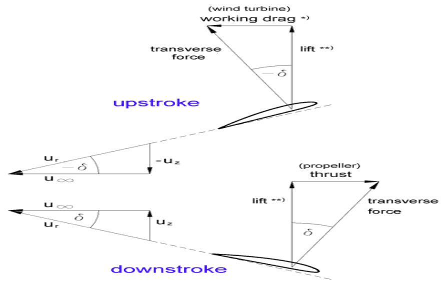

Figure 2 Up stroke And Down stroke action

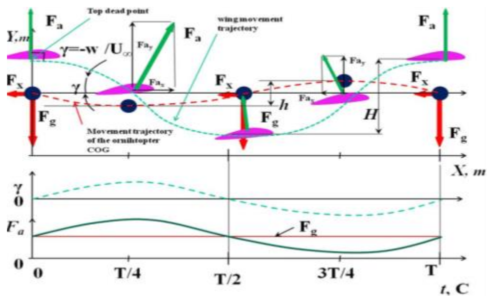

Figure 3 Flight Operating Principle

The parameter has been calculated for the design. After the analysis of 2D design, the 3D design has been created with the respect.

International Journal of Engineering Research & Technology (IJERT)
ISSN: 2278-0181
Vol. 8 Issue 04, April-2019

II. PARAMETERS CALCULATED FOR DESIGNING THE FLAPPING WING UAV

A. Design Parameters

Table I

S. NO	DESIGN PARAMETERS	DENOTION	UNITS	VALUE
1	LENGTH	L	M	0.23
2	WING SPAN	B	M	0.58
3	MASS	M	Kg	0.476
4	WING AREA	S	m^2	0.0745
5	ASPECT RATIO	AR	----------	4.515
6	TORQUE	T	N	0.358
7	WING LOADING	W/S	Kg/m^2	10.836

B. Flight Parameters

a) FREQUENCY

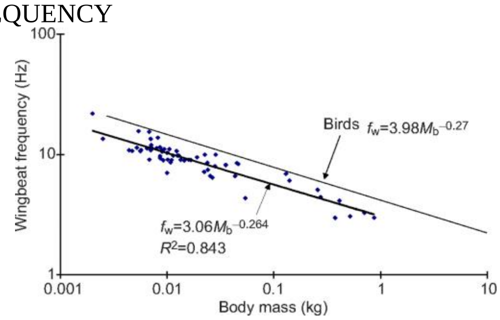

Figure 4. Flapping frequency

$$f = 1.08\ (m1/\ 3\ g1/\ 2\ b{-}1\ S{-}1/\ 4\ \rho{-}1/\ 3)$$

$$f\ (Small\ Birds) = 116.3\ m^{-1/6}$$

$$f\ (Large\ Birds) = 28.7\ m^{-1/3}$$

The frequencies for the parameters designed are

$$\boxed{f = 2.6\ Hz}$$

b) FLIGHT SPEED (U)

The relationship between flight speed & the mass of the bird can be given,

$$U = 4.77\ m^{1/6}$$

Where m is the mass of the bird and U is the Flight speed.

$$\boxed{U = 4.212\ m/s}$$

c) FLAPPING ANGLE (β)

Flapping angle varies β as sinusoidal function. β and its rate is given by following equations.

$$\beta(t) = \beta_{max} \cos 2 \prod f\ t$$

$$\boxed{\beta\ (t) = 22.538^o}$$

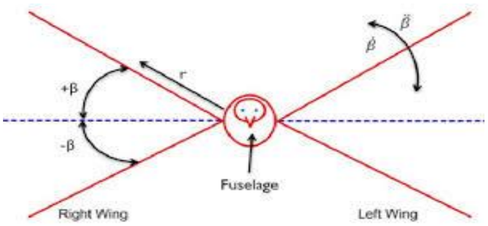

Figure 5 Flapping Angle

d)FLAPPING RATE (β_r)

The equation for flapping rate is given as

$$\beta_r(t) = -2 \prod f\ t \sin 2 \prod f\ t$$

$$\boxed{\beta_r(t) = -374.943\ Hz.s}$$

e) PITCHING RATE (θ)

The angle of climb (slope) is the angle between the horizontal axis and the aircraft flight path.

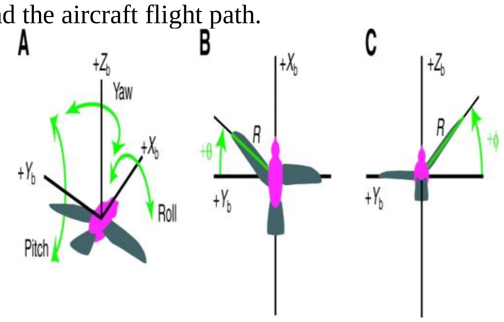

Figure 6. Pitching angle

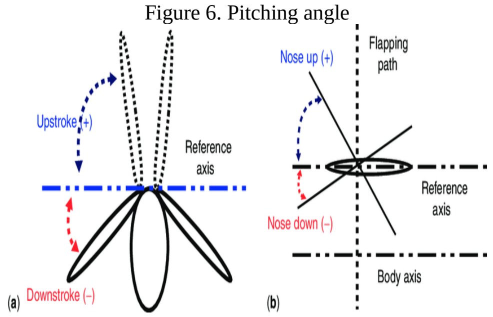

Figure 7. Flapping action

The pitch is the angle between the horizontal axis and the longitudinal axis of the aircraft.

$$\Theta\ (t) = (r(i)/B)\ \theta_o \cos (2 \prod f\ t + \phi)$$

$$\boxed{\Theta\ (t) = 12.5^o}$$

C. Velocity Parameters

a) VERTICAL COMPONENET OF RELATIVE WIND VELOCITY (V_y)

$$V_y = \sin(\delta) + (-r(i).\beta .\cos(\beta)) + (0.75.c.\theta .\cos(\beta)))$$

$$V_y = 2.427 m/s$$

b) HORIZONTAL COMPONENET OF RELATIVE WIND VELOCITY (V_x)

The horizontal component of relative wind velocity is given by

$$V_x = U \cos(\delta) + (0.75.c.\ \theta\ .\sin(\theta))$$

$$V_x = 4.757\ m/s$$

c) RELATIVE VELOCITY (V_{rel})

The relative velocity for the given parameters is given by

$$V_{rel} = (V_x^2 + V_y^2)^{1/2}$$

$$V_{rel} = 5.34\ m/s$$

d) RELATIVE ANGLE (Ψ)

Relative angle between the two velocity components ψ and the effective angle of attack

$$\Psi = \tan^{-1} (V_x / V_y)$$

$$\Psi = 62.97^o$$

D. ANGLE OF ATTACK

a) EFFECTIVE ANGLE OF ATTACK (α_{eff})

Effective Angle of Attack is that part of a given angle of attack that lies between the chord of an airfoil and the effective airflow.

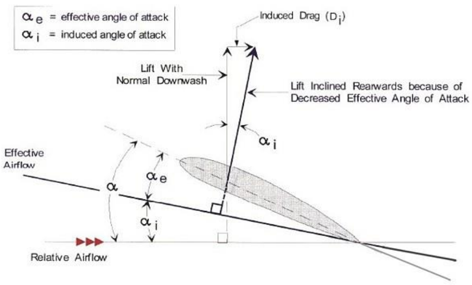

Figure 8. Effective angle of attack

Effective airflow is a line representing the resultant velocity of the disturbed airflow.

$$\alpha_{eff} = \psi + \theta$$

$$\alpha_{eff} = 75.47^o$$

b) RELATIVE ANGLE OF ATTACK (α)

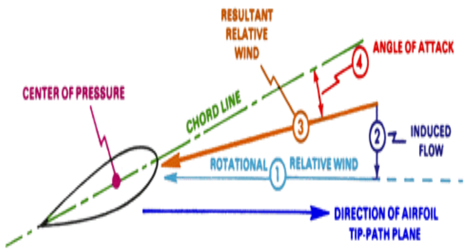

Figure 9. Relative angle of attack

$$\boldsymbol{\alpha = 6^O}$$

c) FLOW RELATIVE ANGLE OF ATTACK (α^I)

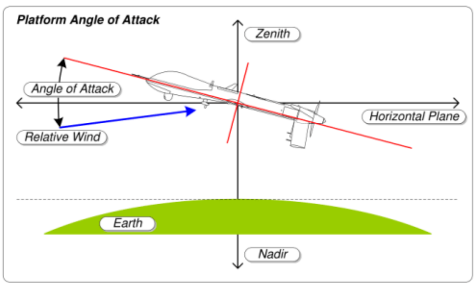

Figure 10. Angle of attack

$$\boldsymbol{\alpha^I = 2.4^O}$$

d) CYCLE ANGLE (Φ)

The cycle angle is given by

$$\boldsymbol{\Phi = 58^o}$$

e) SECTION MEAN PITCH ANGLE (Θ^I)

The section mean pitch angle is given by

$$\Theta^i = 60^o$$

E. FORCE PARAMETERS

a) HORIZONTAL COMPONENT OF FORCE(F_{hor})

The horizontal component of force is given by

$$F_{hor} = dL_c \sin\psi . \cos\delta + dN_{nc} \sin(-\theta) . \cos\delta - dD_d \cos\psi . \cos\delta$$

$$F_{hor} = -1.232 \text{ N}$$

b) VERTICAL COMPONENT OF FORCE (F_{hor})

$$F_{ver} = dL_c \cos\psi . \cos\delta + dN_{nc} \cos(-\theta) . \cos\beta . \cos\delta$$

$$F_{ver} = 0.2777\text{N}$$

c) NORMAL FORCE(N_{nc})

The vertical component of force is given by

$$N_{nc} = 0.306\text{N}$$

F. LIFT PARAMETERS

a) THEODORSON LIFT DEFICIENCY (C (K))

Theodorsen Lift Deficiency factor which is a function of reduced frequency k

$$C(k) = \sqrt{F^2 + G^2}$$

$$F = 1 - \frac{C_1 . k^2}{k^2 + C_2^2}$$

$$G = -\frac{C_1 C_2 k}{k^2 + C_2^2}$$

C_1 *and* C_2 *are given by*

$$C_1 = \frac{0.5\ AR}{(2.32 + AR)}$$

$$C_2 = 0.181 + \frac{0.772}{AR}$$

C (K) = 0.028

b) LIFT COEFFICIENT DUE TO CIRCULATION ($C_{l\text{-}c}$)

The section lift coefficient due to circulation (KuttaJoukowski condition) for flat plate is given by

$$C_{l-c} = 2\pi\, C(k) \sin \alpha_{eff}$$

$$C_{l\text{-}c} = 0.17$$

c) SECTIONAL LIFT (L_C)

The section lift can thus be calculated by

$$L_c = \frac{1}{2} \rho\, V_{rel}^2\, C_{l-c} . c . dr$$

$$L_C = 0.157\text{N}$$

d) INSTANTANEOUS LIFT (L)

The instantaneous lift is given by

$$L = dN \cos\theta + dF_x \sin\theta$$

L = 0.565 N

e) LIFT ALONG SPAN (L_X)

The lift along the span is given by

$$L_X = 1.105\text{N}$$

G. THRUST PARAMETERS

a) INSTANTANEOUS THRUST (T)

The instantaneous thrust is given by

$$T = dF_x \cos\theta - dN \sin\theta$$

T = 0.204 N

b) THRUST ALONG SPAN (T_X)
The thrust along span is given by

T_x = 1.16

H. DRAG PARAMETERS

a) INDUCED DRAG COEFFICIENT (C_{di})

$$C_{di} = \frac{C_{l-c}{}^2}{e\,\pi\,AR}$$

C_{di} = 0.002468

b) INDUCED DRAG (D_i)

$$D_i = \frac{1}{2}\rho\, V_{rel}^2\, C_{di}\, .\, c\, .\, dr$$

D_i = 0.001708 N

c) PARASITE DRAG COEFFICIENT (C_{dp})

$$C_{Dp} = K.\, C_f$$

C_{dp} = 11.1257

d) PARASITE DRAG (D_p)

$$D_p = \frac{1}{2}\rho\, V_{rel}^2\, C_{dp}\, .\, c\, .\, dr$$

D_p = 2.887 N

e) TOTAL DRAG (D_d)

$D_d = D_p + D_i$

D_d = 2.888 N

f) SKIN FRICTIONAL DRAG COEFFICIENT (C_f)

$$C_f = 0.445\,(log_{10}\, Re_{ref})^{-2.58}$$

C_f = 2.529

I. PRESSURE DIFFERENCE BETWEEN UPPER AND LOWER SURFACE

Pressure (symbol: p or P) is the force applied perpendicular to the surface of an object per unit area over which that force is distributed.

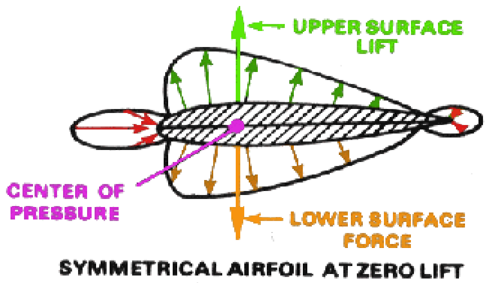

Figure 11. Pressure difference

Gauge pressure is the pressure relative to the ambient pressure.

Δ p = 0.507 BAR

J. POWER

a) POWER INPUT (P_{in})

$$P_{in}(t) = 2\int_0^{\frac{b}{2}} dP_{in}$$

P_{in} = 0.9 W

b) POWER OUTPUT (P_{out})

$$\bar{P}_{out} = \bar{T}U$$

P_{out} = 0.72 W

b) EFFICIENCY (η)

$$\bar{n} = \frac{\bar{P}_{out}}{\bar{P}_{in}}$$

η = 82.22

III. DESIGN

A. SELECTION OF AEROFOIL

The aerofoil to be selected must be similar to the shape of the bird wing.

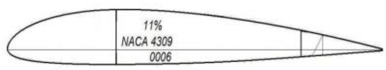

Figure 12. NACA 4309

So on analyzing different aerofoil and finding similarities the NACA 4309 aerofoil is been selected

B. DESIGN OF AEROFOIL

The design of aerofoil in CATIA V5 by importing the coordinates of aerofoil from excel sheet.

Figure 13. Aerofoil

C. CONNECTING RODS

The connecting rod which connects the two gears and two sides of the assembled wing structure which creates the flapping motion.

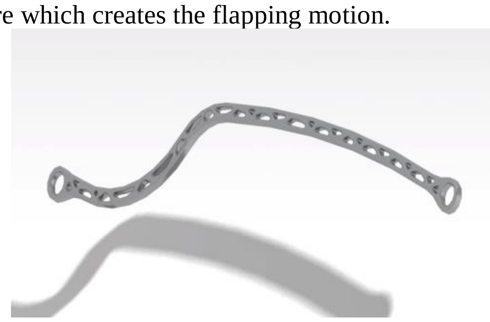

Figure 14. Connecting rod

International Journal of Engineering Research & Technology (IJERT)
ISSN: 2278-0181
Vol. 8 Issue 04, April-2019

D. WING SKELETON STRUCTURE

The aerofoil and different crank that are used to connect the aerofoil to construct the skeleton structure of the wing which is driven by the gear mechanism.

Figure 15. Wing skeleton structure

E. RUNNING GEAR

The running gear is the main gear which is attached to the wing skeleton structure which is connected to the connecting rod to make the flapping motion.

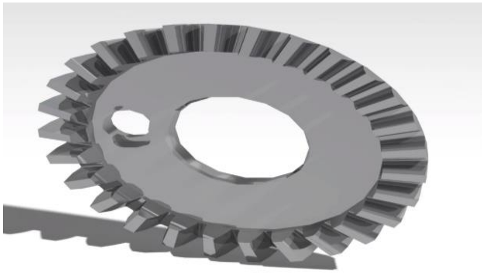

Figure 16. Running gear

F. PINION

The pinion gear is the gear which drives the main gear. The gear is attached to the key which is driven by rotating the key.

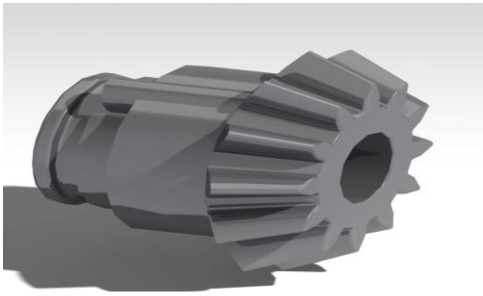

Figure 17. Pinion

G. BODY DESIGN

The design of body parts is designed according to the shape of the birds analyzed.

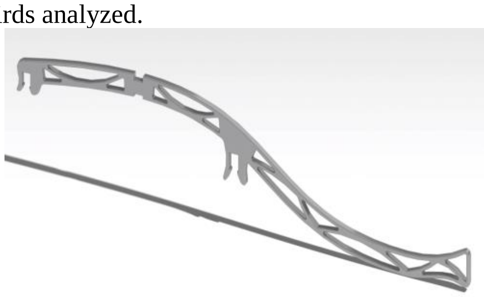

Figure 18 Side Body

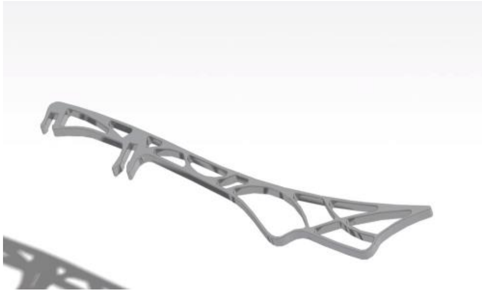

Figure 19. Top body

H. ASSEMBLED WING STRUCTURE ALONG WITH GEAR

The wing structure after the assembling of aerofoil and connecting rod is then connected with running gear and pinion.

Figure 20. Assembled gear with wing

I. ASSEMBLING OF OTHER PARTS

After assembling the gear and pinion to the wing skeleton structure the body structure is merged with the wing structure.

Figure 21. Assembled structure

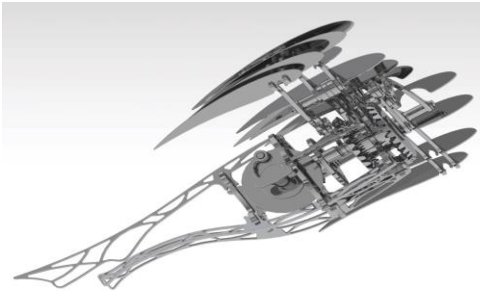

Figure 22. Assembled structure side view

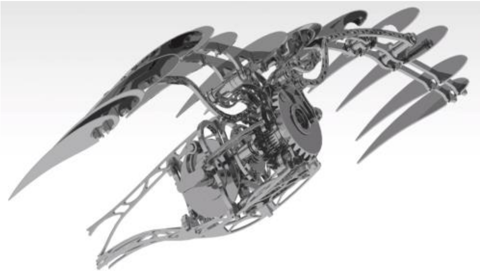

Figure 23. Assembled structure cross view

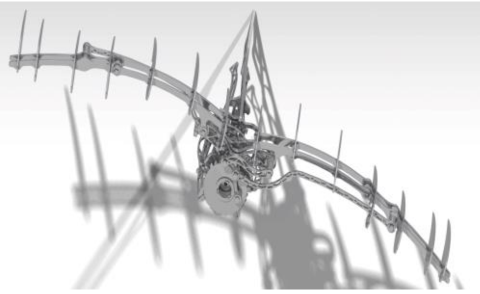

Figure 24. Assembled structure front view

J. SHEET METAL APPLICATION

Figure 24 Applied Skin Over The Wing

IV. RESULTS

A. Dynamic velocity

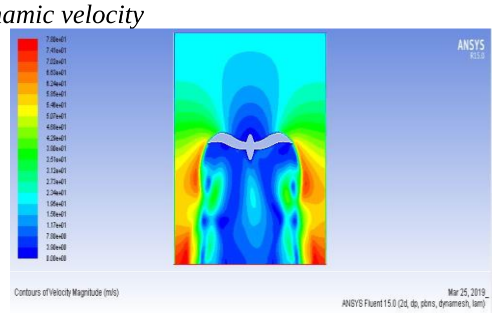

Figure 25 Velocity

B. Mesh Deformation X Velocity

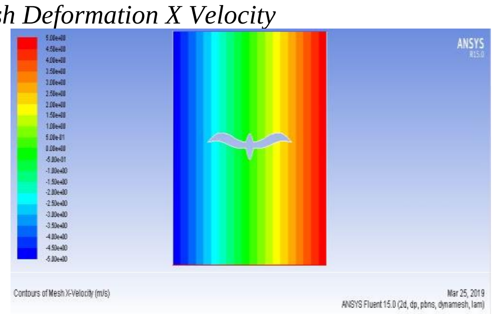

Figure 26 Mesh X Velocity

C. Mesh Deformation Y Velocity

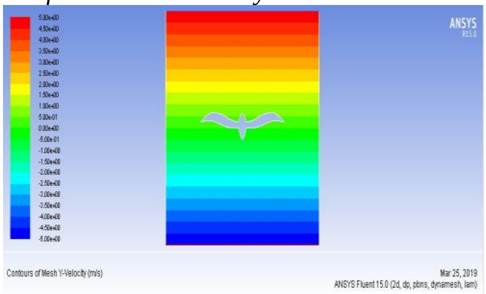

Figure 27 Mesh Y Velocity

D. Relative X Velocity

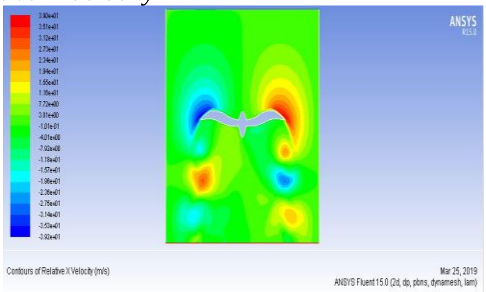

Figure 28 Relative X Velocity

E. Relative Y Velocity

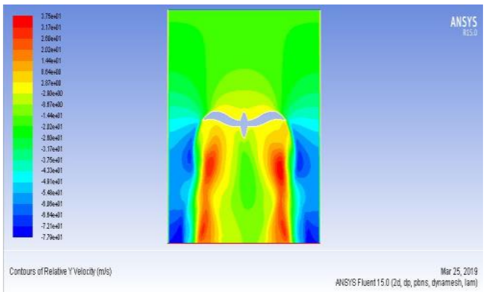

Figure 29 Relative Y Velocity

F. Vorticity

Figure 30 Vorticity

G. Tangential Velocity

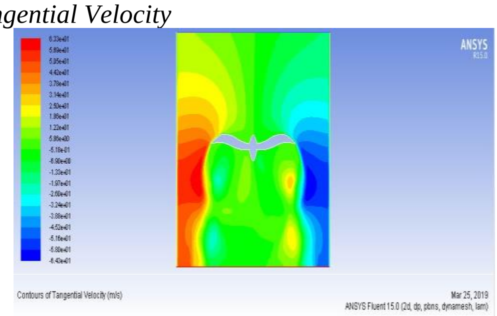

Figure 31 Tangential Velocity

International Journal of Engineering Research & Technology (IJERT)
ISSN: 2278-0181
Vol. 8 Issue 04, April-2019

H. Radial velocity

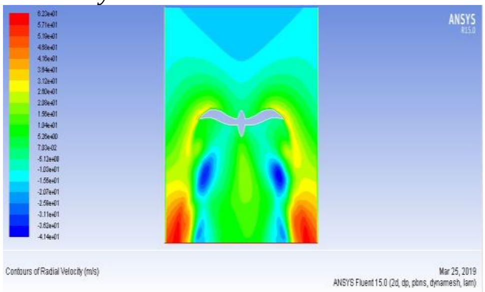

Figure 32 Radial Velocity

I. X Velocity

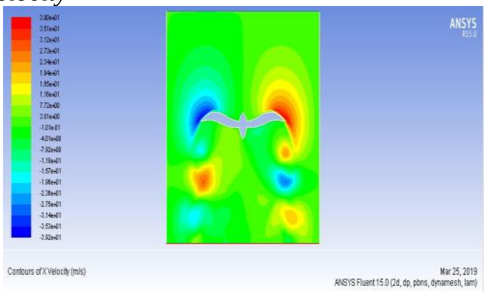

Figure 33 X Velocity

J. Y Velocity

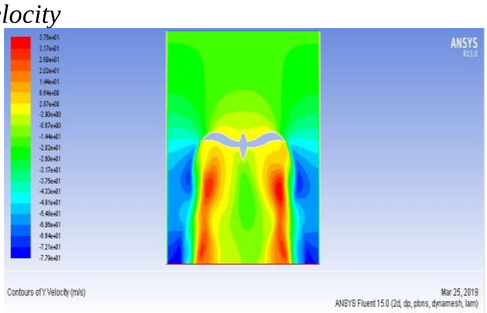

Figure 34 Y Velocity

K. Velocity Angle

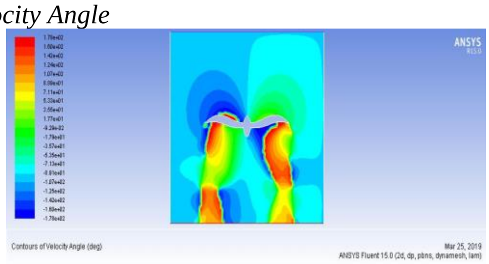

Figure 35 Velocity Angle

L. Cell Reynolds number

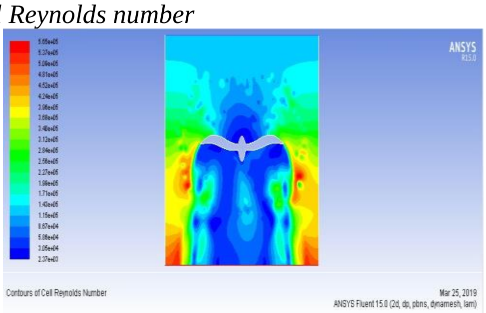

Figure 36 Reynolds Number

M. Dynamic Pressure

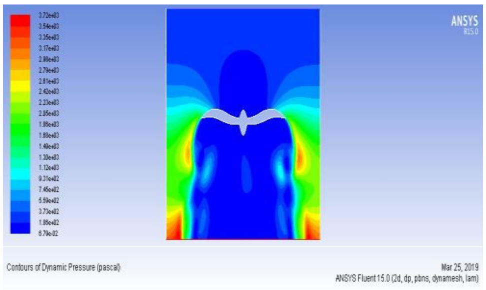

Figure 37 Dynamic Pressure

N. Total Pressure

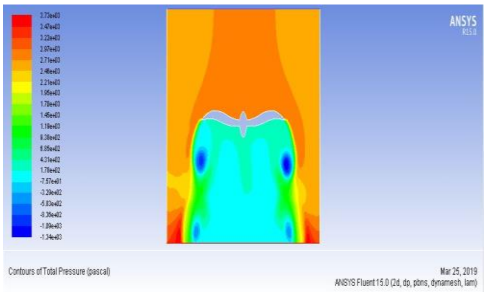

Figure 38 Total Pressure

O. Density

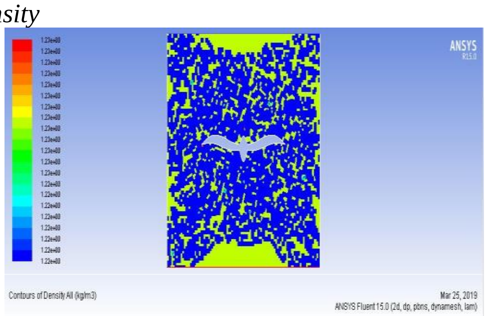

Figure 39 Density

P. Temperature

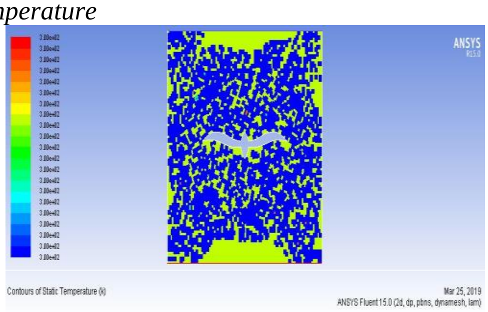

Figure 40 Temperature

Q. Enthalpy

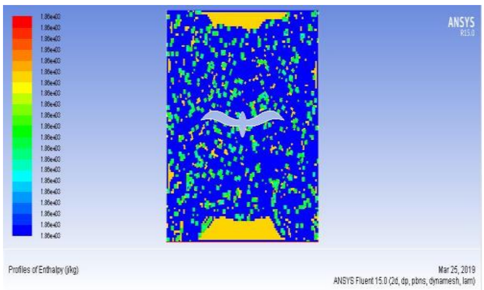

Figure 41 Enthalpy

R. Wall Temperature

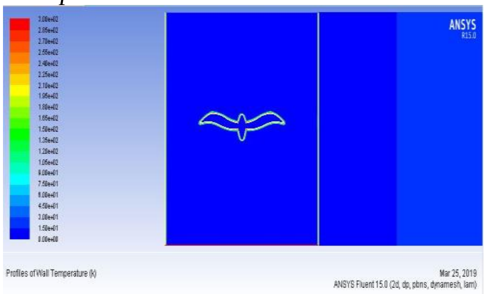

Figure 42 Wall Temperature

S. Entropy

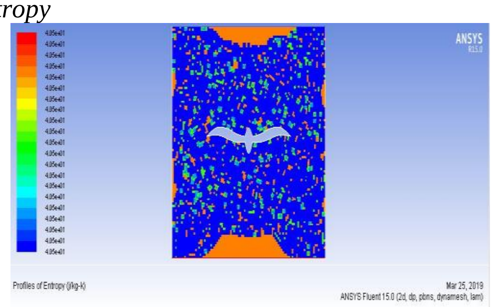

Figure 43 Entropy

T. Total Energy

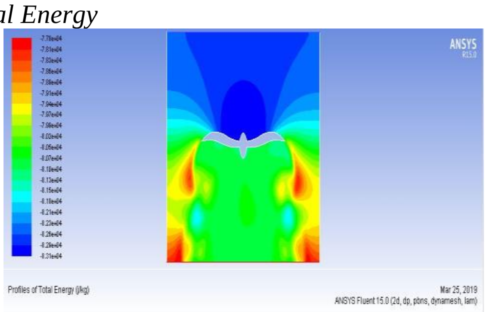

Figure 44 Total Energy

U. Internal Energy

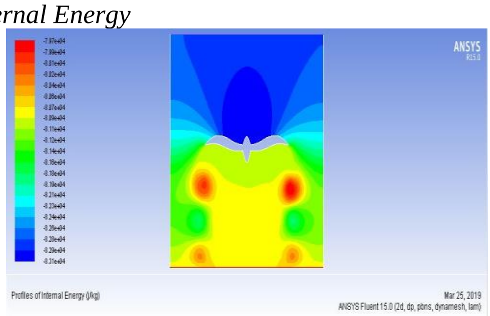

Figure 45 Internal Energy

V. Total Enthalpy

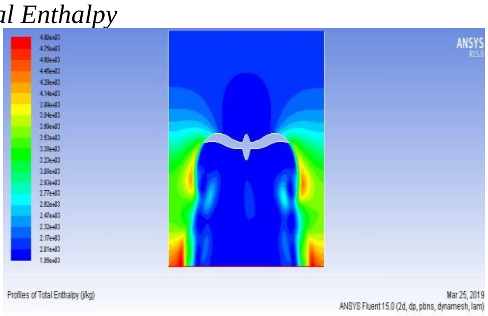

Figure 46 total enthalpy

V. CONCLUSION

In this paper the flapping wing UAV has been designed and analysed to evaluate its aerodynamic performance in the airflow. Using GAMBIT, the 2D structure has been designed and analysed by FLUENT. The results show that this structure have good aerodynamic design with standard flow parameters. With the reference of 2D design, the 3D structure has been with all its interior parts and gear systems. The results obtained from the FLUENT analysis clearly proves and ensures that it can work better with the flow over it.

REFERENCES

[1] Zachary John Jackowski, Design and Construction of Autonomous Ornithopter, June 7, 2009
[2] Akshay Bhargava, Apoorv Bhargava, Saurabh Kr. Jangid , *Ornithopter Development and Operation*, March 24,2015
[3] M Afzaal Malik, Farooq Ahmad, Effect of Different Design Parameters On Lift, Thrust and Drag of an Ornithopter, July 2,2010
[4] Jithin M P, Jude Olivero, Naveen M Nair, Sarath R ,Vinod Yeldho Baby, *Design of Ornithopter Flapping Wing Mechanism* , April 04,2018
[5] Alphan Canga, Michael Delia, Alexander Hyman, Angela Nagelin, *Fluidic Muscle Ornithopter*, March 27, 2015
[6] Bo-Hsun Chen, Li-Shu Chen, Yueh Lu, Zih-Jie Wang and Pei-Chun Lin,
Design of a Butterfly Ornithopter, July 7,2016
[7] K. P. Preethi Manohari Sai, K. Bharadwaj, K. Ravi Teja, Kalyan Dagamoori,
Kasiraju Venkata Sai Tarun, Vishnu Vijayan , *Design, Fabrication and Testing Of Flapping Wing Micro Air Vehicle,* January 16, 2016
[8] S. Adjerid and J. E. Flaherty, A moving FEM with error estimation and refinenment for
1-D time dependent PDEs, SIAM J. Numer. Anal. 23 (1986), 778{795
[9] A moving-mesh FEM with local refinement for parabolic PDEs, Comput. Meth.
Appl. Mech. Engrg. 55 (1986), 3{26
[10] D. A. Anderson, Adaptive mesh schemes based on grid speeds, AIAA Paper 83-1931 (1983),
311
[11] Equidistribution schemes, poisson generators, and adaptive grids, Appl. Math. Comput. 24 (1987), 211{227
[12] D.C. Arney and J.E. Flaherty, A two-dimensional mesh moving technique for time dependent
partial differential equations, J. Comput. Phys. 67 (1986), 124{144
[13] B.N. Azarenok, Realization of a second-order Godunov's scheme, Comput. Meth. in Appl.
Mech. and Engin. 189 (2000), 1031{1052
[14] Variational barrier method of adaptive grid generation in hyperbolic problems of
gas dynamics, SIAM J. Numer. Anal. 40 (2002), 651{682
[15] B.N. Azarenok, S.A. Ivanenko, and T. Tang, Adaptive mesh redistribution method based on
Godunov's scheme, Commun. Math. Sci. 1 (2003), 152{179
[16] B.N. Azarenok and T. Tang, Reactive flow calculations on moving meshes, 2005, To appear
in J. Comput. Phys
[17] M.J. Baines, Moving Finite Elements, Oxford University Press, 1994
[18] Grid adaptation via node movement, Appl. Numer. Math. 26 (1998), 77{9}